Supporting Information

Singlet oxygen production and biological activity of hexanuclear chalcocyanide rhenium cluster complexes $[\{Re_6Q_8\}(CN)_6]^{4-}$ (Q is S, Se or Te)

Anastasiya O. Solovieva,[†,‡] Kaplan Kirakci,[§] Anton A. Ivanov,[†,‖] Pavel Kubát,[▽] Tatiana N. Pozmogova,[‡,O] Svetlana M. Miroshnichenko,[‡] Elena V. Vorontsova,[#] Anton V. Chechushkov,[†] Kristina E. Trifonova,[⊥] Maria S. Fufaeva,[†] Evgeniy I. Kretov,[∀] Yuri V. Mironov,[‖,O,∀] Alexander F. Poveshchenko,[‡] Kamil Lang,[§*] Michael A. Shestopalov[†,‡,‖,O*]

[†]Research Institute of Experimental and Clinical Medicine, 2 Timakova st., 630117 Novosibirsk, Russian Federation

[‡]Research Institute of Clinical and Experimental Lymphology – Branch of the ICG SB RAS, 2 Timakova st., 630060 Novosibirsk, Russian Federation

[§]Institute of Inorganic Chemistry of the Czech Academy of Sciences, v.v.i., Husinec-Řež 1001, 250 68 Řež, Czech Republic

[‖]Nikolaev Institute of Inorganic Chemistry SB RAS, 3, Acad. Lavrentiev Ave., Novosibirsk 630090, Russian Federation

[▽]J. Heyrovský Institute of Physical Chemistry of the Czech Academy of Sciences, v.v.i., Dolejškova 3, 182 23 Praha 8, Czech Republic

[O]Novosibirsk State University, 2 Pirogova Str., Novosibirsk 630090, Russian Federation

[#]The Institute of Molecular Biology and Biophysics, 2/12 Timakova st., 630117 Novosibirsk, Russian Federation

[⊥]The State Research Center of Virology and Biotechnology VECTOR, 630559 Koltsovo, Russian Federation

[∀]Meshalkin Siberian Federal Biomedical Research Center, 15 Rechkunovskaya st., 630055 Novosibirsk, Russian Federation

Corresponding Authors

*Kamil Lang, E-mail: lang@iic.cas.cz
*Michael A. Shestopalov, E-mail: shtopy@niic.nsc.ru

Content

Influence of NaN_3 on triplet state kinetics and transient absorption spectra of $K_4[\{Re_6Q_8\}(CN)_6]$

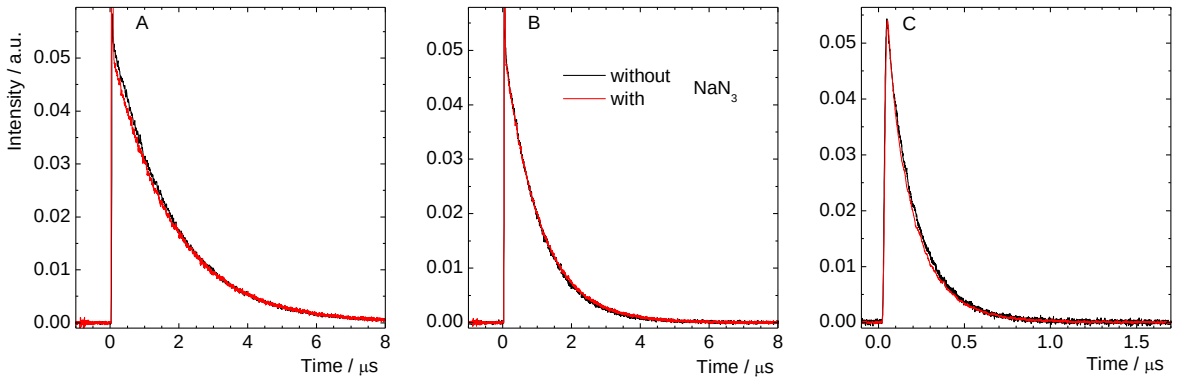

Figure S1. Influence of NaN_3 on the luminescence decay curves of K_4-**1** (A), K_4-**2** (B), and K_4-**3** (C) recorded at 720 nm in oxygen-saturated D_2O. The samples were excited at 425 nm, red curves were recorded in the presence of NaN_3.

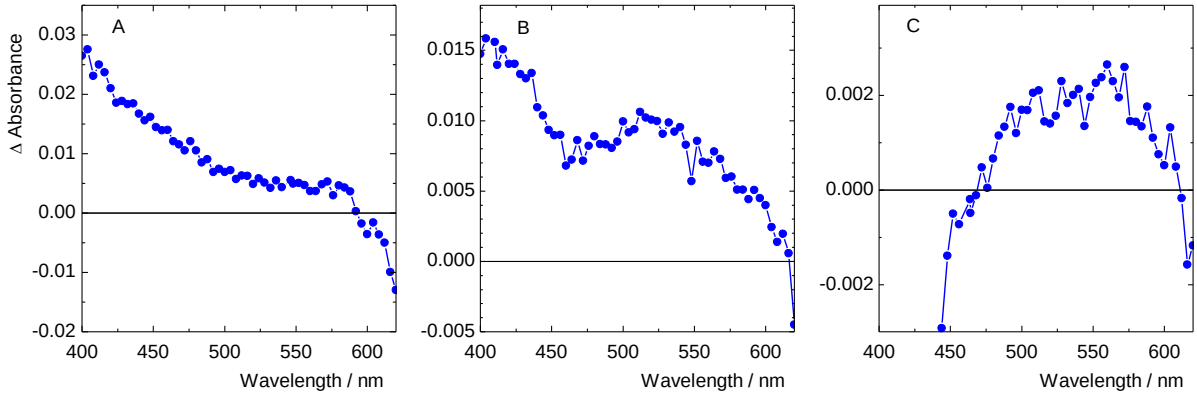

Figure S2. Transient absorption spectra of K_4-**1** (A), K_4-**2** (B), and K_4-**3** (C) upon excitation at 355 nm in H_2O.

Luminescence decay curves of $K_4[\{Re_6Q_8\}(CN)_6]$ in oxygen-, air-, or argon-saturated H_2O/D_2O

A

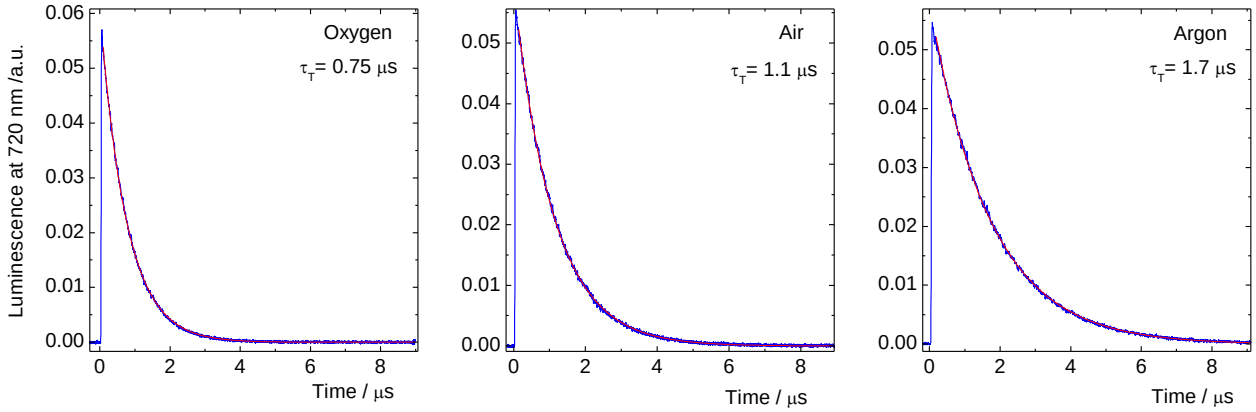

B

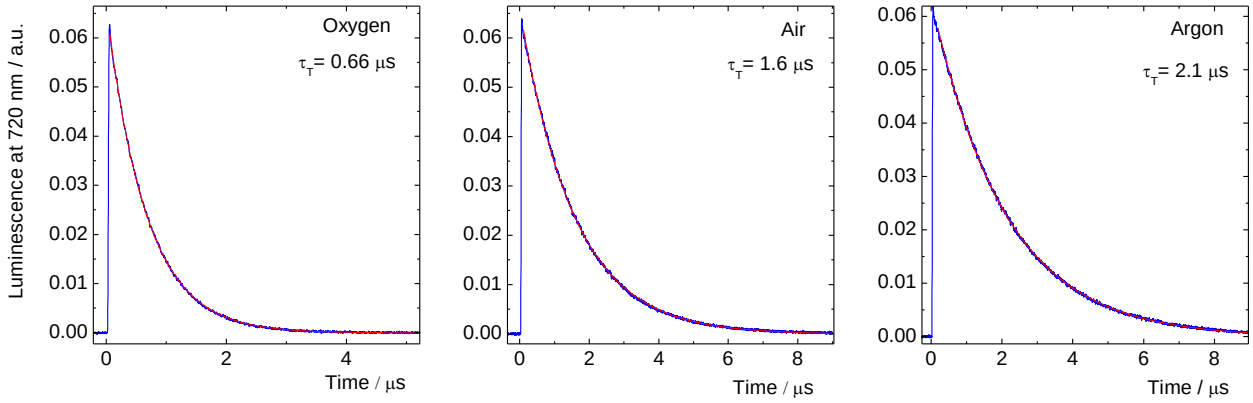

C

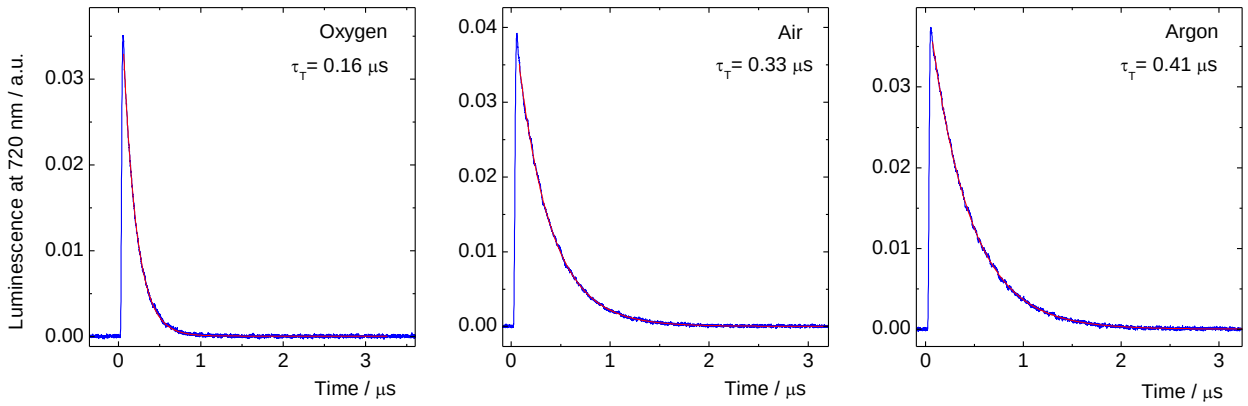

Figure S3. Luminescence decay curves of K_4-**1** (A), K_4-**2** (B), and K_4-**3** (C) recorded at 720 nm in oxygen-, air-, or argon-saturated H_2O. The samples were excited at 425 nm; red lines represent corresponding monoexponential fits.

A

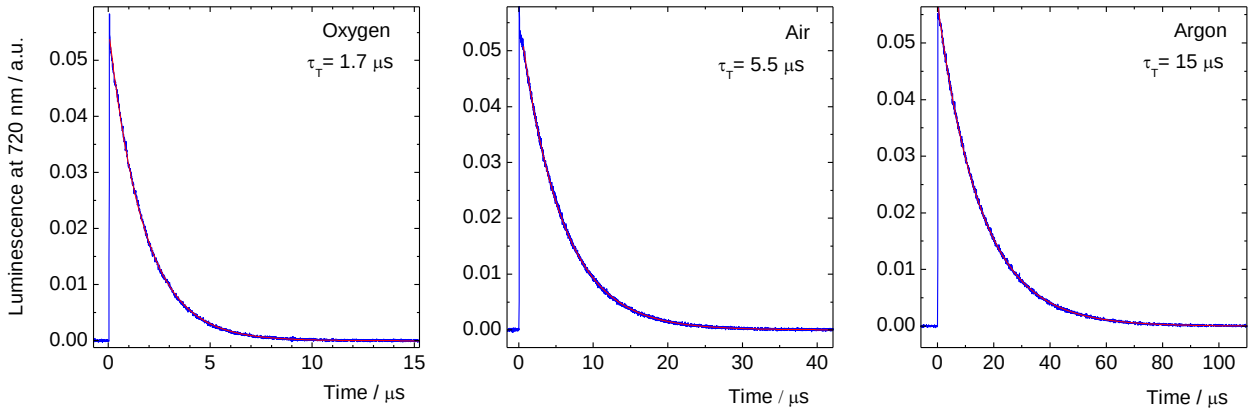

B

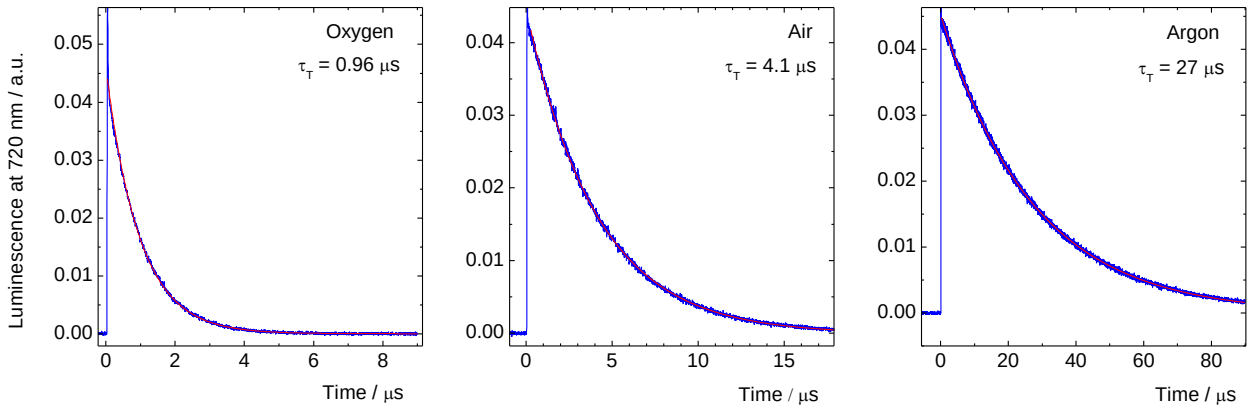

C

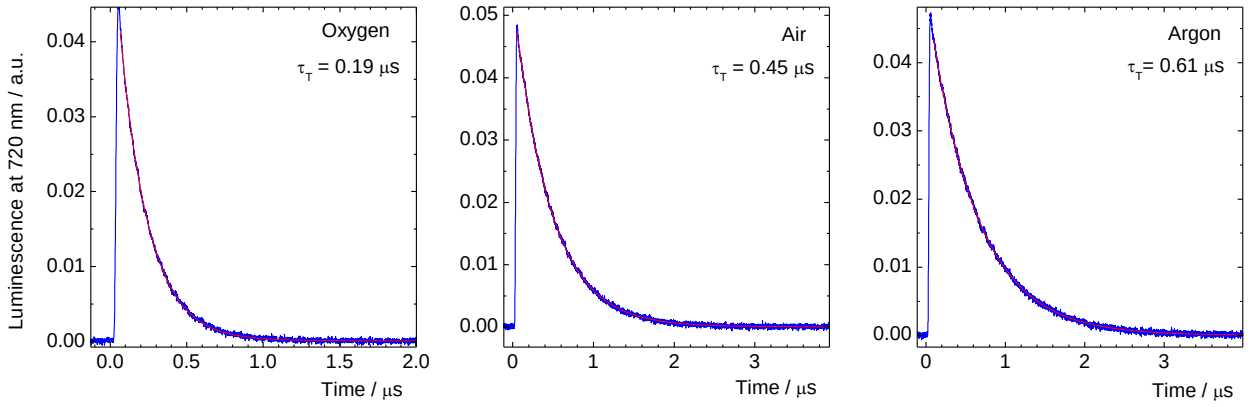

Figure S4. Luminescence decay curves of K_4-**1** (A), K_4-**2** (B), and K_4-**3** (C) recorded at 720 nm in oxygen-, air-, or argon-saturated D_2O. The samples were excited at 425 nm; red lines represent corresponding monoexponential fits.

Transient absorption decay curves of $K_4[\{Re_6Q_8\}(CN)_6]$ in oxygen-, air-, or argon-saturated H_2O

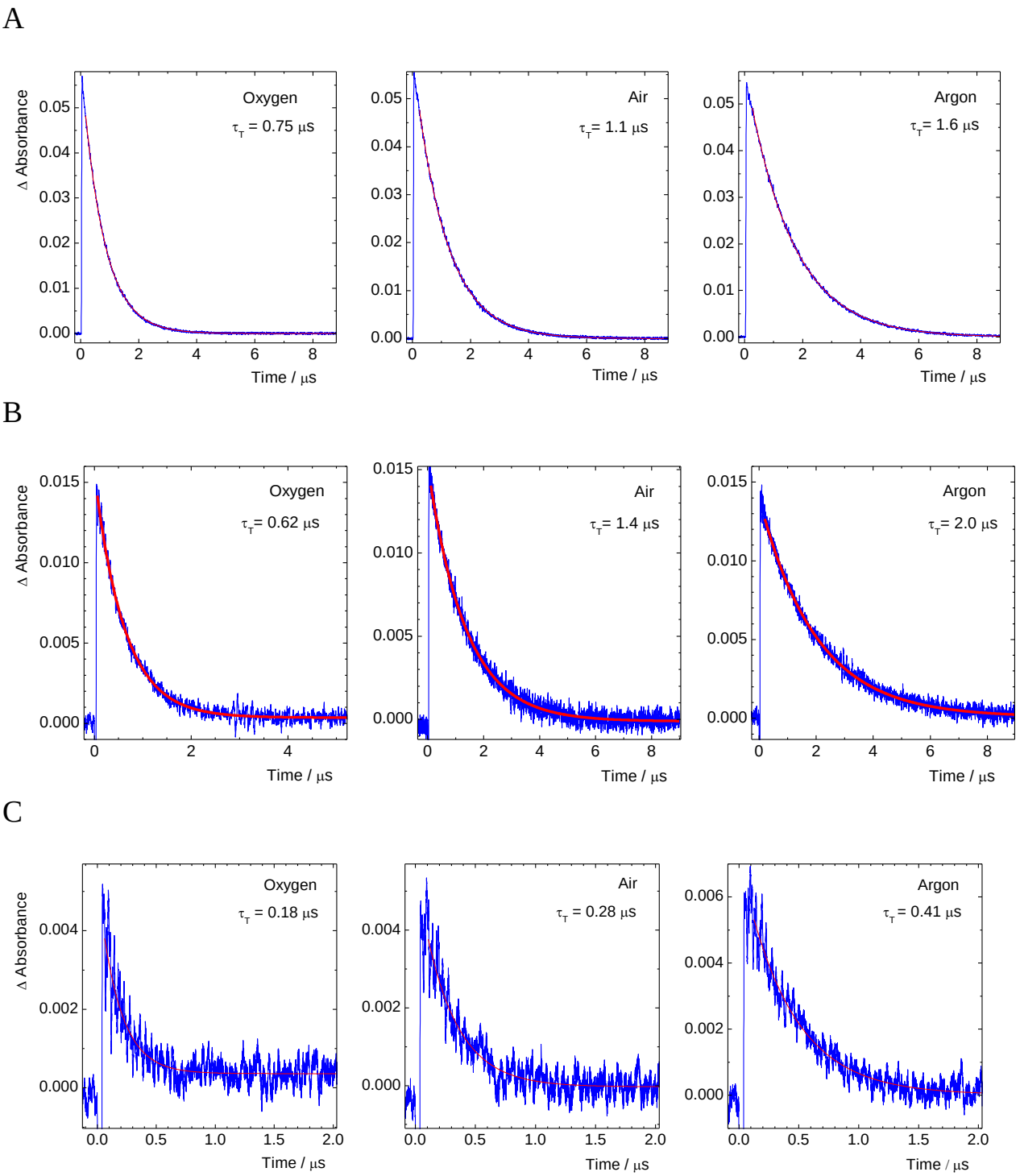

Figure S5. Transient absorption decay curves of K_4-**1** (A), K_4-**2** (B), and K_4-**3** (C) in oxygen-, air-, or argon-saturated H_2O. The traces were recorded at 520 nm (K_4-**1**, K_4-**2**) and 560 nm (K_4-**3**) upon excitation at 355 nm; red lines represent corresponding monoexponential fits.

Stern Volmer analysis of the triplet state quenching by oxygen

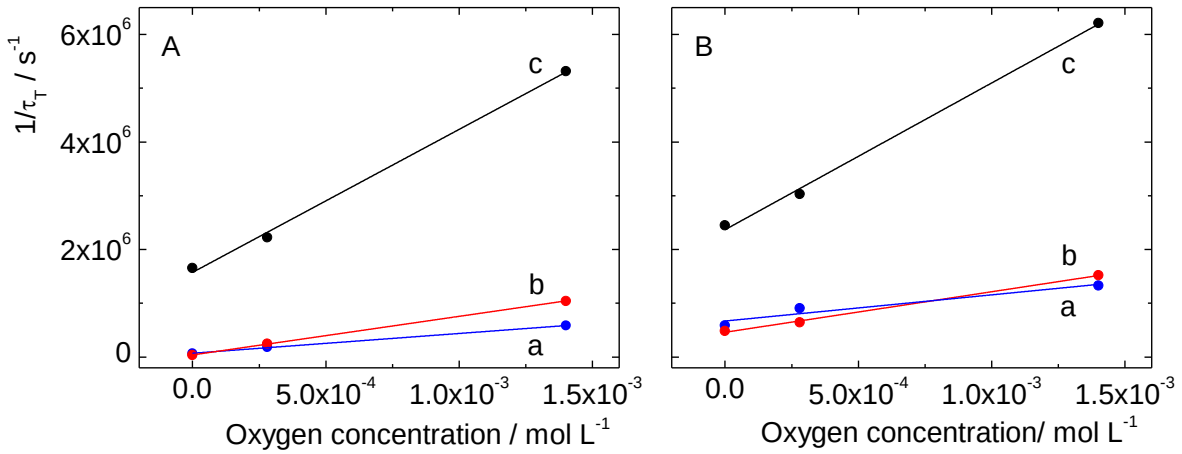

Figure S6. Stern Volmer analysis of the triplet state quenching of K_4-**1** (a), K_4-**2** (b), and K_4-**3** (c) by oxygen in D_2O (A) and H_2O (B).

Luminescence of $O_2(^1\Delta_g)$ after excitation of $K_4[\{Re_6Q_8\}(CN)_6]$ and comparison with a standard porphyrin photosensitizer

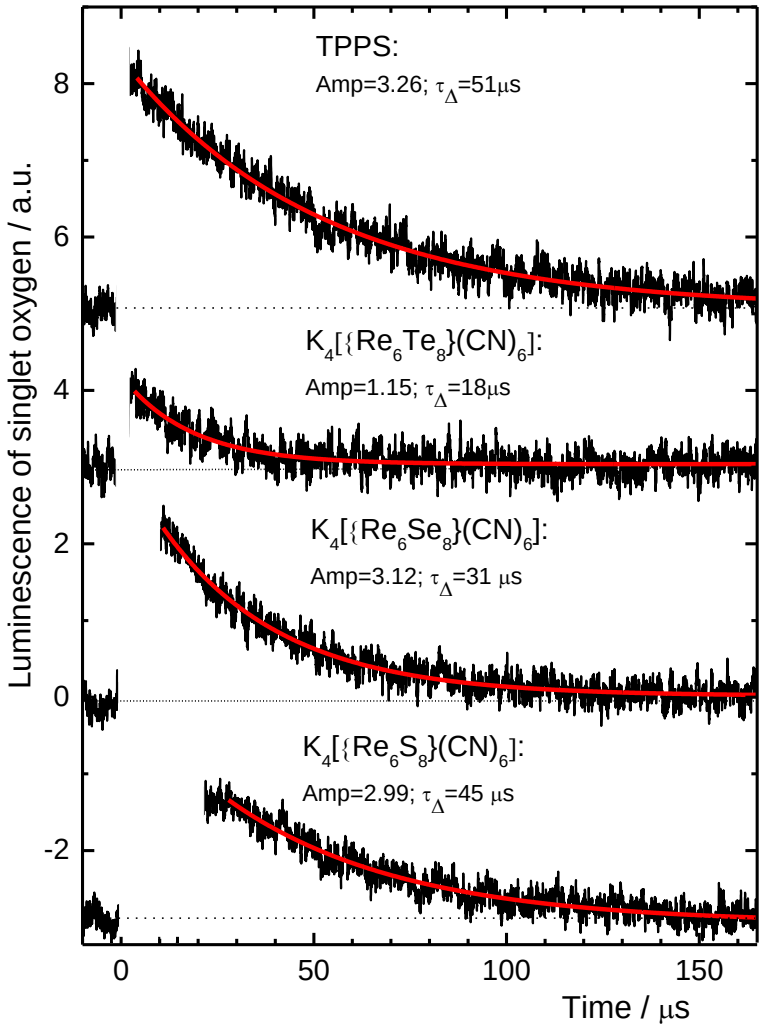

Figure S7. Luminescence of $O_2(^1\Delta_g)$ at 1270 nm after excitation of $K_4[\{Re_6Q_8\}(CN)_6]$ and 5,10,15,20-tetrakis(4-sulfonatophenyl)porphyrin (TPPS) at 425 nm in oxygen- saturated D_2O. Red lines represent single exponential fits into experimental data.

Z-stacked confocal fluorescence microscopy images

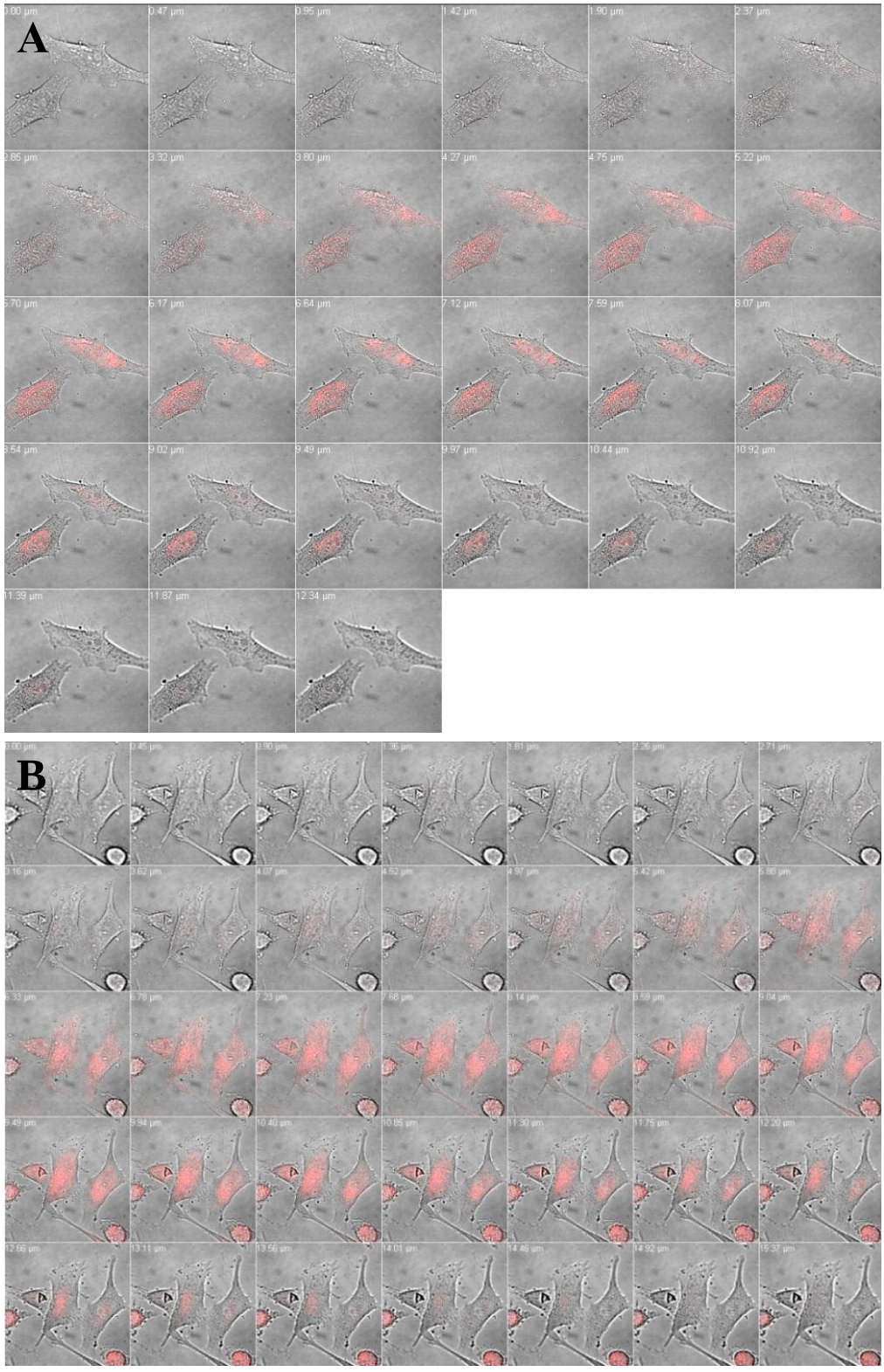

Figure S8. Z-stacked image of Hep-2 cells incubated with $Na_4[\{Re_6Q_8\}(CN)_6]$ (Q = S or Se) by confocal fluorescence microscopy: A) Hep-2 cells incubated with $Na_4[\{Re_6S_8\}(CN)_6]$, 100 μM; B) Hep-2 cells incubated with $Na_4[\{Re_6Se_8\}(CN)_6]$, 100 μM. ×100 microscope objective.

Radiopacity vs. concentration, X-ray computed tomography and angiography images of $Na_4[\{Re_6Q_8\}(CN)_6]$ (Q = S, Se, Te) solutions of indicated concentrations

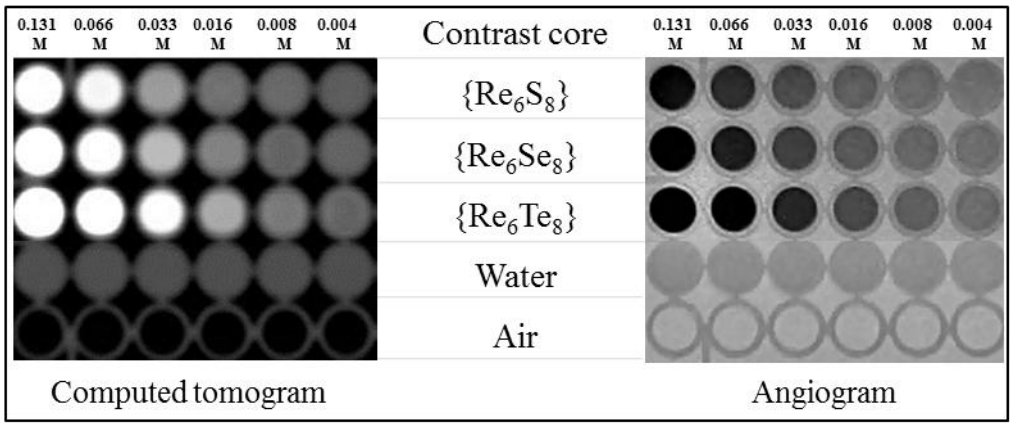

Figure S9. X-ray computed tomography and angiography images of H_2O solutions of $Na_4[\{Re_6Q_8\}(CN)_6]$ (Q = S, Se, Te); concentrations varied from 4 to 131 mM. H_2O and air were used as references.

Table S1. Radiopacity of $Na_4[\{Re_6Q_8\}(CN)_6]$ aqueous solutions in the Hounsfield unit (HU) scale.

Cluster	Radiopacity, HU					
	0.131 M	0.066 M	0.033 M	0.016 M	0.008 M	0.004 M
Na_4-**1**	2859 ± 239	1641 ± 74	747 ± 48	346 ± 26	263 ± 18	150 ± 14
Na_4-**2**	3804 ± 343	2027 ± 183	1032 ± 95	505 ± 28	223 ± 20	211 ± 9
Na_4-**3**	6250 ± 607	3386 ± 194	1754 ± 126	895 ± 26	428 ± 25	226 ± 35
Water	14 ± 3	9 ± 5	5 ± 4	8 ± 3	6 ± 5	8 ± 5
Air	–963 ± 78	–977 ± 48	–984 ± 34	–991 ± 25	–988 ± 27	–987 ± 30

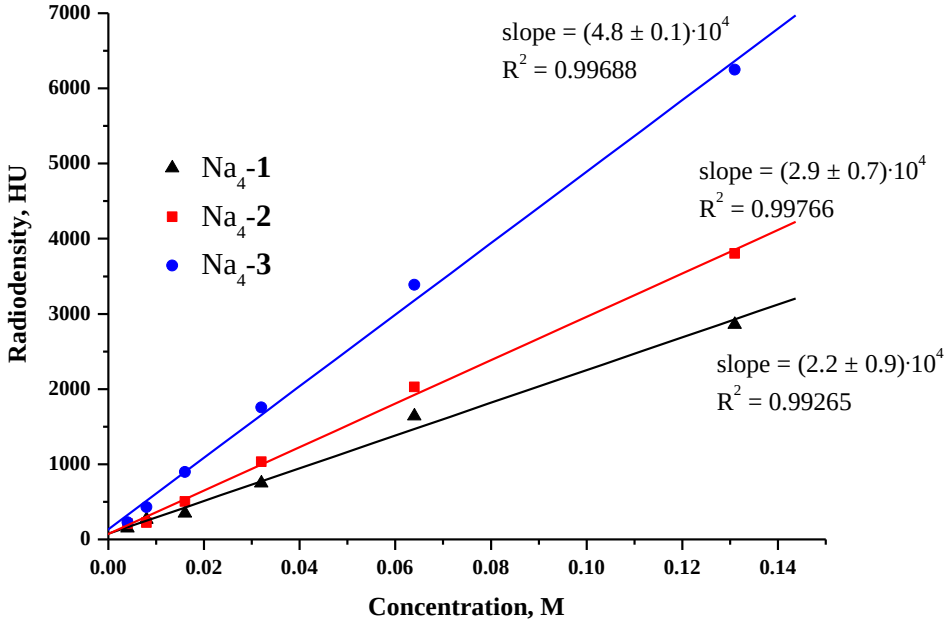

Figure S10. Dependence of radiopacity of Na_4-**1**, Na_4-**2** and Na_4-**3** water solutions in the Hounsfield unit scale on concentrations.